Lithium delays progression of amyotrophic lateral sclerosis

Francesco Fornai*†‡, Patrizia Longone§, Luisa Cafaro†, Olga Kastsiuchenka*, Michela Ferrucci*, Maria Laura Manca¶, Gloria Lazzeri*, Alida Spalloni§, Natascia Bellio‖, Paola Lenzi*, Nicola Modugno†, Gabriele Siciliano¶, Ciro Isidoro‖, Luigi Murri¶, Stefano Ruggieri†, and Antonio Paparelli*

*Department of Human Morphology and Applied Biology, and ¶Department of Neuroscience, Clinical Neurology, University of Pisa 56100 Pisa, Italy; †Istituto Neurologico Mediterraneo, Istituto Di Ricovero e Cura a Carattere Scientifico Neuromed, 86077 Pozzilli (IS), Italy; §Molecular Neurobiology Unit, Santa Lucia Foundation, 00179 Rome, Italy; and ‖Department of Medical Sciences, University of Novara, 28100 Novara, Italy

Edited by Thomas C. Südhof, University of Texas Southwestern Medical Center, Dallas, TX, and approved December 21, 2007 (received for review August 24, 2007)

ALS is a devastating neurodegenerative disorder with no effective treatment. In the present study, we found that daily doses of lithium, leading to plasma levels ranging from 0.4 to 0.8 mEq/liter, delay disease progression in human patients affected by ALS. None of the patients treated with lithium died during the 15 months of the follow-up, and disease progression was markedly attenuated when compared with age-, disease duration-, and sex-matched control patients treated with riluzole for the same amount of time. In a parallel study on a genetic ALS animal model, the G93A mouse, we found a marked neuroprotection by lithium, which delayed disease onset and duration and augmented the life span. These effects were concomitant with activation of autophagy and an increase in the number of the mitochondria in motor neurons and suppressed reactive astrogliosis. Again, lithium reduced the slow necrosis characterized by mitochondrial vacuolization and increased the number of neurons counted in lamina VII that were severely affected in saline-treated G93A mice. After lithium administration in G93A mice, the number of these neurons was higher even when compared with saline-treated WT. All these mechanisms may contribute to the effects of lithium, and these results offer a promising perspective for the treatment of human patients affected by ALS.

autophagy | clinical study | G93A mice | morphological analysis

ALS is a devastating neurodegenerative disorder with no effective treatment that usually leads to death within 3–5 years from diagnosis (11 months for the bulbar form) (1). ALS occurrence is primarily (90%) sporadic, while only 10% is familial (fALS). Approximately 20% of fALS are due to mutations of the gene coding for the enzyme copper–zinc superoxide-dysmutase (SOD1) (2). Transgenic mice over expressing the human mutant SOD1 develop a pathology that is very similar to that seen in ALS patients [see supporting information (SI) *Text* for a comparison]. Studies in animal models or *in vitro* led to the identification of a variety of alterations in ALS motor neurons (MN) (1, 3, 4); however, other cells in the spinal cord besides MN are affected (5–8). For instance, a class of interneurons die either before or concomitantly with MN, as found in mice (9, 10) and postulated in humans for Renshaw-like cells (11). Again, glial cells participate in the deleterious interplay leading to MN degeneration (6–8).

After the generation of the SOD1 ALS mouse models, attempts have been made to find effective treatments. However, so far, none of these trials has led to effective clinical outcomes.

Lithium is a compound used as a mood stabilizer, which is neuroprotective in a variety of disease models (12, 13), such as brain ischemia (14) and kainate toxicity (15). The ability of lithium to promote autophagy, through the inhibition of the inositol-monophosphatase 1 (16–18), together with the protective effects of autophagy in neurodegeneration (19–22), prompted us to test the neuroprotective effects of lithium in the G93A ALS mouse model. Based on the promising data, we obtained in mice we quickly moved into a clinical trial, which is now at the end of its second year.

Results

Effects of Lithium on Disease Duration and Survival in G93A Mice. G93A male mice were treated daily with lithium carbonate (1 mEq/kg, i.p.), starting at 75 days of age. Lithium treatment prolonged the mean survival time from 110.8 ± 5.0 days ($n = 20$) to 148 ± 4.3 ($n = 20$, ≈36% of the life span of these mice; Fig. 1*a*; $P < 0.001$) and, most importantly, increased disease duration (from a mean of 9 days to >38 days, >300%; Fig. 1*b*; $P < 0.05$) compared with the G93A mice treated with saline. Even when lithium treatment was started at the onset of motor symptoms, the increase in disease duration was still comparable (data not shown). More specifically, lithium delayed the onset of paralysis and limb adduction (Fig. 1*c*) and significantly improved additional tests we report in SI Fig. 6, such as rotarod, grip strength, and stride length.

Effects of Lithium Treatment on Motor Neuron Survival (Lamina IX of Lumbar and Cervical Spinal Cord and Brainstem Motor Nuclei). These effects were accompanied by a reduced loss of lumbar MN at 90 days of age (SI Fig. 7). However, at the end of disease (which occurred later following lithium), the number of alpha-MN within lumbar lamina IX of the G93A mice treated with lithium was comparable to that found in the saline-treated mice that had died previously (SI Fig. 8). However, even at this stage, we detected a disease modifying effect of lithium. This consisted of (*i*) preservation of the size of MN (SI Fig. 8 *d* and *e*); (*ii*) preservation of MN number and size in those areas [i.e., cervical spinal cord (SI Fig. 9) or the nucleus ambiguous (SI Fig. 10)], which degenerate later compared with lumbar lamina IX (23, 24); (*iii*) decreased astrocytosis (SI Fig. 11); and (*iv*) decreased alpha-synuclein, ubiquitin, and SOD1 aggregation (see SI Fig. 6 and *Discussion* in *SI Text*).

Effects of Lithium Treatment on the Renshaw-Like Cell Area (Lamina VII). Lamina VII contains a larger number of interneurons, defined as Renshaw cells, which form a collateral circuit that

Author contributions: F.F., P. Longone, C.I., L.M., S.R., and A.P. designed research; O.K., M.F., M.L.M., G.L., A.S., N.B., P. Lenzi, N.M., and G.S. performed research; L.C., M.F., M.L.M., G.L., P. Lenzi, G.S., C.I., L.M., S.R., and A.P. analyzed data; and F.F. and P. Longone wrote the paper.

The authors declare no conflict of interest.

This article is a PNAS Direct Submission.

Freely available online through the PNAS open access option.

‡To whom correspondence should be addressed. E-mail: f.fornai@med.unipi.it.

This article contains supporting information online at www.pnas.org/cgi/content/full/0708022105/DC1.

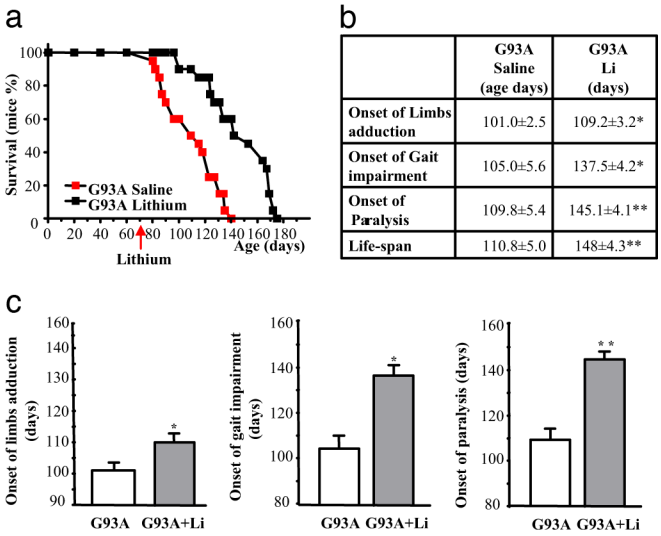

	G93A Saline (age days)	G93A Li (days)
Onset of Limbs adduction	101.0±2.5	109.2±3.2*
Onset of Gait impairment	105.0±5.6	137.5±4.2*
Onset of Paralysis	109.8±5.4	145.1±4.1**
Life-span	110.8±5.0	148±4.3**

Fig. 1. Effects of lithium treatment on the lifespan and neurological symptoms of G93A mice. (*a*) Survival curve for saline- and lithium-treated G93A mice. Lithium carbonate (1 mEq/kg, daily, i.p.) treatment significantly increased the survival time of G93A mice compared with saline-treated mice. (*b*) Effects of lithium on specific symptoms, such as hind limb adduction, gait impairment, and the onset of severe paralysis. (*c*) Symptomatic effects and prolongation of the life span induced by lithium. Values represent the mean ± SEM of 10 mice per group in two different experiments (total *N* per group = 20). Comparison was made by using ANOVA with Sheffe's post hoc analysis. *, $P \leq 0.05$ compared with G93A mice administered saline. **, $P \leq 0.001$ compared with G93A mice administered saline.

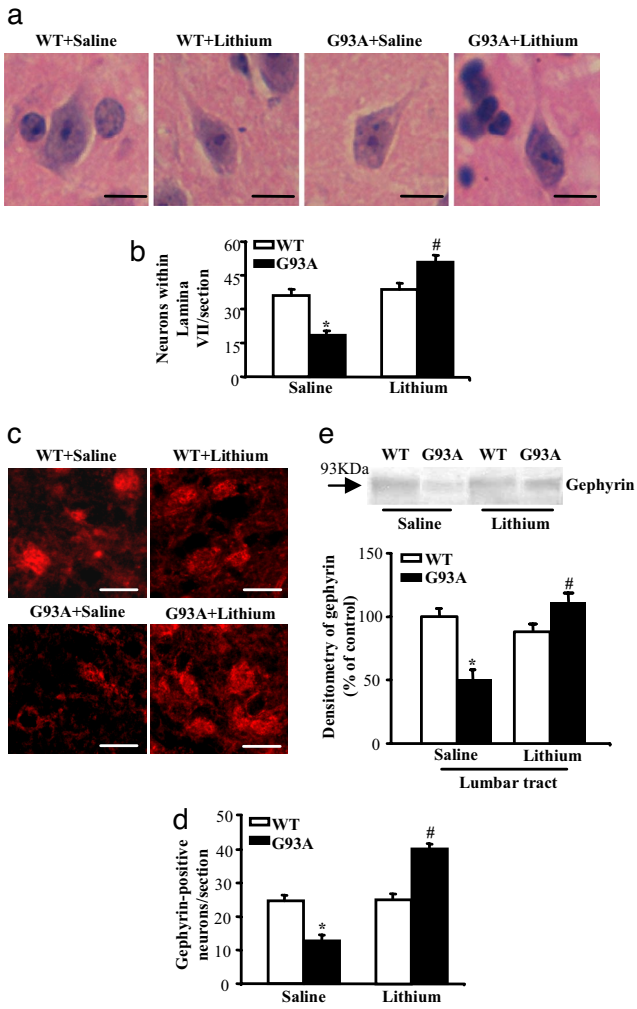

Fig. 2. Neuroprotective effects of lithium on medium-size lamina VII neurons. (*a*) Shows representative micrographs of those H&E-stained lamina VII neurons that were selected for the count based on size specificity (diameter ranging from 10 to 20 μm). (*b*) Graph indicates the severe loss of these neurons in G93A mice, which exceeded the loss of MN. Remarkably, the G93A mice treated with lithium showed a much higher number of lamina VII medium-size neurons even compared with saline-treated WT mice. (*c–e*) These results were confirmed by gephyrin immunostaining, as shown here and by all of the staining procedures summarized in SI Fig. 16. Counts represent the mean ± SEM of 62,000 cells per group (3,100 per mouse in groups of 20 mice). Comparison among groups was made by using one-way ANOVA. *, $P \leq 0.05$ compared with WT saline-treated group. #, $P \leq 0.001$ compared with G93A saline-treated groups. (Scale bars, 17 μm.)

inhibits MN (25). Renshaw neurons are defined by electrophysiological properties but typically stain for gephyrin and calbindin 28k. Therefore, we used the term Renshaw-like neurons to refer to these cells. We focused on these neurons based on findings by Martin *et al.* (9), who showed that, in G93A mice, interneurons begin to die before MN; further, pioneer electrophysiological studies suggested an early impairment of Renshaw cells in ALS patients (11). We found that neurons within lamina VII of G93A mice were severely decreased (more than MN, 50% loss, from 36 ± 2.97 to 18.53 ± 1.84; Fig. 2 *a* and *b*). Remarkably, lithium administration led to an increase in the number of these neurons, which became more abundant even when compared with control mice (131% and 100%, respectively). This net increase in neuron number occurred only when lithium was administered to G93A mice; no such effect occurs in WT (Fig. 2*b*). All of the staining procedures performed to visualize these neurons within lamina VII confirmed these results: H&E (131% of controls), gephyrin (137% of controls; Fig. 2 *c* and *d*), NeuN (132% of controls; SI Fig. 12 *a* and *b*) and calbindin 28k (126% of controls; SI Fig. 13 *a* and *b*). Immunoblotting confirmed all these staining (Fig. 2*e* and SI Figs. 7*c* and 13*c*). Moreover, the procedure of BrdU incorporation at immunofluorescence (SI Fig. 14) and by using ImmunoGold TEM (SI Fig. 15) confirmed the increase in calbindin 28k positive neurons in lamina VII. This is summarized in SI Fig. 16. The increase in neuron number produced by lithium in the spinal cord is disease dependent, because it did not occur in WT. Lithium is known to produce neurogenesis in physiological conditions in the hippocampus (26) but not in the spinal cord. However, in the absence of lithium, occurrence of neurogenesis in the spinal cord of G93A mice is uncertain, and, when occurring (27), it does not produce a net increase in neuron number compared with controls. In the present study, we combined lithium administration with the ongoing disease state. This combination may be necessary to enhance the neurogenetic effects, leading to a robust increase in the number of neurons (see *Discussion* in *SI Text*).

Lithium Treatment Rescues Spinal Cord Mitochondria and Facilitates the Clearance of Alpha-Synuclein, Ubiquitin, and SOD1. In ALS, alpha-synuclein and ubiquitin accumulate in affected neurons (9, 28–30). Lithium treatment reduces the accumulation of alpha-synuclein in both MN of lamina IX (SI Fig. 17*a*) and in neurons of lamina VII (SI Fig. 17 *b* and *c*). Similarly, lithium reduces ubiquitin (SI Figs. 18 and 19), and SOD1 aggregates in MN (SI Fig. 20).

In G93A mice, MN undergo vacuolization, a process defined as "slow necrosis" (9), in whichthey appear to be filled with vacuoles (4, 9) due to mitochondrial swelling (Fig. 3 and SI Figs. 8 and 21). Lithium decreases vacuolization (Fig. 3*f* and *h* and SI Fig. 21) and

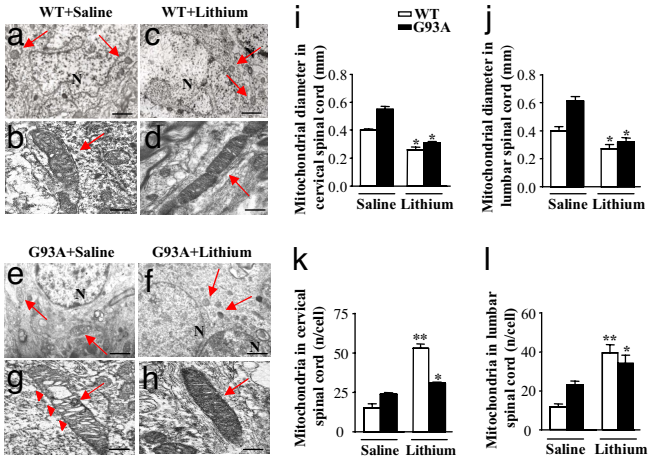

Fig. 3. Effects of lithium administration on motor neurons mitochondria *in vivo*. (*a–h*) Representative pictures of mitochondria (arrows) in MN from the spinal cord of WT mice treated with saline (*a* and *b*) or lithium (*c* and *d*) and from G93A mice treated with saline (*e* and *g*) or lithium (*f* and *h*). (*g*) In G93A mice treated with saline, TEM shows mitochondrial vacuolization (arrowheads). (*f* and *h*) This vacuolization is consistently absent in mitochondria of G93A mice treated with lithium. (*d* and *h–j*) Lithium decreases the size of mitochondria both in WT and G93A mice (*d* and *h*, respectively) both in the cervical (*i*) and lumbar (*j*) spinal cord. (*k* and *l*) Lithium increases the number of mitochondria both in cervical (*k*) and lumbar (*l*) MN both in WT and G93A. Values are the mean ± SEM. Comparison between groups was made by using one-way ANOVA. *, $P \leq 0.05$ compared with saline-treated mice. **, $P \leq 0.01$ compared with saline treated mice. (Scale bars: *a*, *c*, *e*, and *g*, 1.8 μm; *b*, *d*, *f*, and *h*, 0.25 μm.)

normalizes mitochondrial size (Fig. 3 *i* and *j* and SI Fig. 21). Moreover, lithium increases the number of normal mitochondria in both WT and G93A mice. This was counted at ultrastructural level (Fig. 3 *k* and *l*) and confirmed by semiquantitative RT-PCR (SI Fig. 22) *in vivo*. We replicated this effect by cytofluorimetric counts of the mitochondria labeled with MitoTracker Red and MitoTracker Green and by Western blot analysis of cytochrome C (SI Fig. 23 *a–c*) in SH-SY5Y cells and primary spinal cord cultures (SI Fig. 23 *d* and *e*). The increase in mitochondria we found in the spinal cord confirms what recently found in endothelial cells (31). This is very encouraging, considering that the loss of mitochondria may be a risk for drugs acting as autophagy enhancers.

Lithium Increases the Number of Autophagic Vacuoles. At the ultrastructural level, we found degenerating mitochondria within authophagic vacuoles and whorl-like autophagosomes within G93A MN (Fig. 4). This led us to explore the hypothesis that lithium may improve MN survival by activating autophagy (18). We stained spinal cord samples with monodansylcadaverine (MDC), a fluorescent dye that incorporates selectively into autophagolysosomes (32). When lithium was administered, there was a marked increase in autophagy vacuoles as confirmed by ImmunoGold-conjugated autophagy markers, such as beclin or the microtubule-associated protein 1 light chain 3 (LC3) (Fig. 4 *e* and *f*). In fact, the number of beclin and LC3 positive vacuoles was increased by lithium (Fig. 4 *g* and *h*). This effect was confirmed by counting autophagosomes in SH-SY5Y cells stably transfected with LC3 (33). By counting these markers and the vacuoles detected at phase contrast, we found that lithium and rapamycin (used as a positive control for autophagy) increased vacuoles formation (Fig. 4 *i–l*, arrows) and GFP-LC3 fluorescence (Fig. 4 *m–p*), whereas asparagine (an amino acid known to down regulate authopagy; see ref. 34) antagonized the effects of lithium. Induction of autophagy by lithium was matched by increased expression of PTEN (the phosphatase acting on PIP3)

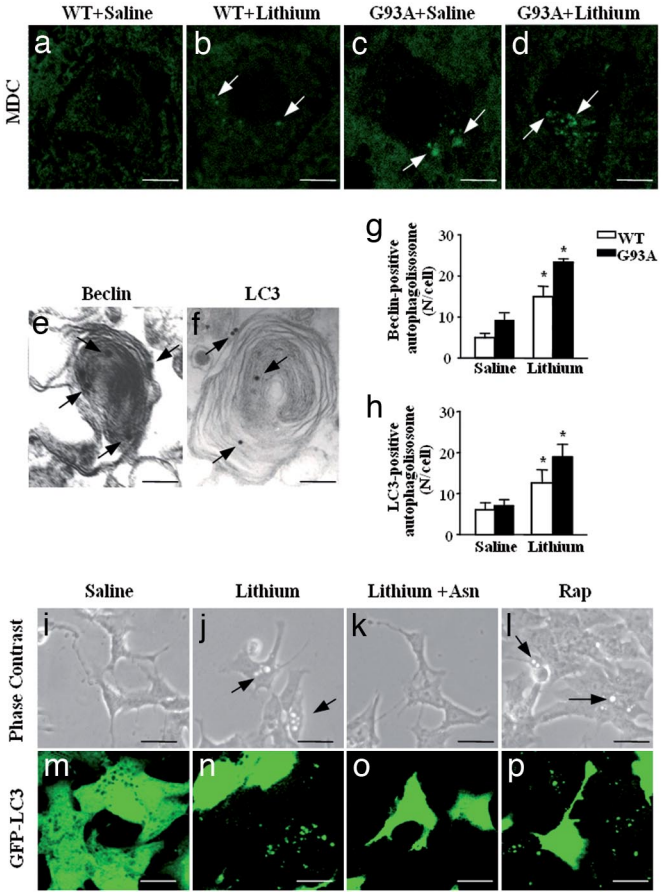

Fig. 4. Effects of lithium on autophagy *in vivo* and *in vitro*. (*a–d*) MDC-positive small vacuoles in the lumbar spinal cord of WT (*a* and *c*, arrows) and G93A mice (*b* and *d*, arrows). (*e*) Representative picture of beclin immunostained vacuoles in the cytoplasm of alpha MN from a G93A lithium-treated mouse. The ImmunoGold particles (20 nm) are localized on both the membrane (that surround the core) and the electrondense core (arrows). (*f*) LC3 immunostaining is present on a larger membranous structure; the ImmunoGold particles (20 nm) are randomly localized (arrows). (*g*) The count of beclin immunostained structures shows a marked effect of lithium in MN both WT and G93A mice. (*h*) Likewise, LC3 immunopositive vacuoles increase significantly in G93A and WT mice administered lithium. (*i–l*) Phase-contrast microscopic images of lithium-induced accumulation of vacuoles in SH-SY5Y cells exposed or not for 72 h to 1 mM lithium (*j*), or lithium plus 50 mM asparagine (Asn) (a slight autophagy blocker acting downstream of lithium) (*k*), or 400 nM rapamycin (Rap) (*l*). Arrows point to cytoplasmic vacuoles that accumulate in cells treated with lithium or Rap (a known autophagy inducer). No vacuolization was observed in control (*i*) or lithium plus Asn-treated cells. (*m–p*) A parallel experiment was performed with transfected SH-SY5Y cells stably expressing the GFP-LC3 chimeric fluorescent protein. The images clearly show that both lithium (*n*) and rapamycin (*p*) change the cytoplasmic diffuse fluorescence pattern of GFP-LC3 to a punctuated pattern indicative of autophagosome formation. Asparagine (*o*) inhibited the effect of lithium on GFP-LC3 localization. *, $P < 0.05$ compared with saline. (Scale bars: *a–d*, 14 μm; *e*, 0.1 μm; *f*, 0.08 μm; *i–l*, 20 μm; *m–p*, 50 μm.)

and a marked reduction in the SER473 phosphorylation of Akt (data not shown). These data confirm the role of autophagy in neurodegeneration (35) and indicate a powerful effect of chronic lithium administration.

Effects of Lithium on Spinal Cord Cultures from G93A Transgenic Mice. If autophagy deficiency causes neurodegeneration in ALS, then its blockade is expected to worsen MN death. To test this hypotheses, we treated spinal cord cultures with the autophagy inhibitor 3-MA (36). MN survival was evaluated by counting

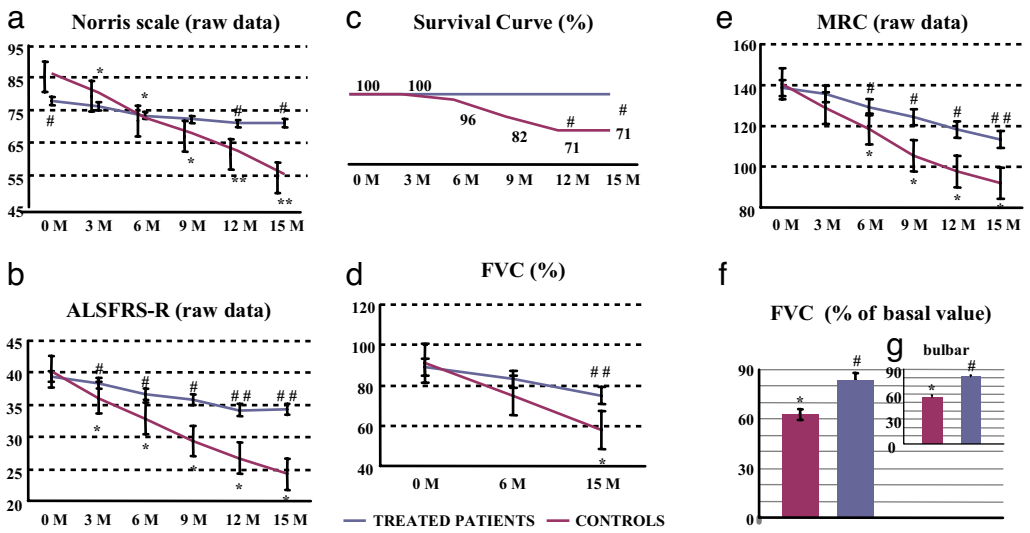

Fig. 5. Effects of lithium treatment on disease symptom progression and survival in patients with ALS. (*a*, *b*, *d*, and *e*) Symptoms progression (evaluated every 3 months) in controls (riluzole-treated) and treated patients (lithium plus riluzole-treated patients) expressed as raw data, using the Norris (*a*) and ALSFRS-R (*b*) rating scales and FVC (*d*) and MRC (*e*). There was no significant progression in the lithium-treated patients at any time interval apart from the last two evaluations using the MRC scale. In the riluzole-treated patients, symptoms progressed significantly starting at 3 or 6 months (depending on the scale). (*c*) Survival curve as normalized data shows the percentage of patients surviving over the 15 months of treatment in the riluzole and lithium groups. None of the patients died in the lithium-treated group; however, in the control group, although the patients had comparable disease severity at enrollment, ≈30% died. Intra- and intergroup analyses were performed by unpaired *t* test or ANOVA followed by the Bonferroni post hoc test. (*f*) Shows the breakdown between treated and control patients for FVC. (*g*) Shows the breakdown between groups for FVC (calculated at 1 month before death) in those patients affected by the bulbar form. *, $P < 0.05$, **, $P < 0.01$ compared with baseline value. #, $P < 0.05$; ##, $P < 0.01$ compared with control patients.

SMI32-positive neurons after drug treatment compared with NT cultures (SI Fig. 24 *a–f*). 3-MA alone (5 mM for 2 h) increased G93A MN death by 58% compared with NT G93A MN and by 51% compared with lithium-treated G93A MN (SI Fig. 24*g*). Moreover, 3-MA treatment significantly increased SMI32-positive MN death in cultures from G93A compared with WT, thus supporting a vulnerability of the autophagy pathway in ALS degeneration (SI Fig. 24*g*). When 3-MA was given 2 h before lithium treatment (18 h, 1 mM), the latter could no longer counteract the effects of 3-MA, confirming that lithium neuroprotection occurs, at least partially, through an autophagic route (SI Fig. 24*g*). As found *in vivo*, lithium administration (18 h) increased gephyrin-positive G93A neurons dose-dependently up to 136% (SI Fig. 24*j*). We further tested the protective effects of lithium against kainate, because G93A MN are highly vulnerable to excitotoxicity (37), which is also a mechanism involved in the neurodegeneration of ALS (1). Lithium (1 mM) given 20 min before kainate (100 μM 15 min) fully protected G93A SMI32-positive neurons (SI Fig. 25 *a* and *b*).

Clinical Trial. The previous results led us to translate the use of lithium carbonate to human patients affected by ALS. Recruitment began in October 2005. Typically, compliance was high or moderate for most individuals. There were no significant differences in demographic variables between groups (mean age and standard error in the treated group, 66.9 ± 1.9 vs. 70.3 ± 1.6 years; mean age at the ALS onset, 63.8 ± 1.7 vs. 67.1 ± 1.7). Similar baseline values between groups for ALSFRS-R scale, Norris scale, forced vital capacity (FVC), and Medical Research Council were selected.

When we measured the progression of the disability score in the group treated with lithium, ANOVA test for repeated measures did not show any statistical difference according to the Norris scale (basal value, 79.4 ± 2.8; final value, 71.0 ± 3.9; Fig. 5*a*) and ALSFRS-R scale (basal value, 39.9 ± 1.2; final value, 34.3 ± 2.3; Fig. 5*b*). Remarkably, all patients treated with lithium were alive at the end of the study. By contrast, in the group receiving riluzole only, 29% of subjects did not survive (Fig. 5*c*). This difference was significant at 12 and 15 months.

Assessment of disease progression with objective measurements such as the pulmonary function (FVC) provided similar data. In fact, FVC did not progress significantly (basal value, 89.0 ± 2.6; final value, 74.9 ± 3.6; Fig. 5*d*). The only significant progression compared with baseline values was observed for MRC but only at the end of the follow up (138.5 ± 1.6; final value, 113.4 ± 4.9; $P < 0.05$; Fig. 5*e*). No significant decrement in the Short Form Health Survey-36 (SF-36) scale for quality of life was detected during the 15 months of lithium administration (96.2 ± 2.0 vs. 93.4 ± 2.1).

These data indicate that subjects receiving lithium progressed very slowly in the disease during the 15 months of the follow-up. By contrast, in patients receiving only riluzole, the Norris scale significantly decreased (86.6 ± 2.1 vs. 55.3 ± 3.2, $P < 0.01$), starting from the 3rd month ($P < 0.05$) (Fig. 5*a*). Similar results were found for ALSFRS-R score, which significantly decreased ($P < 0.01$) (basal value, 40.2 ± 0.8; final value, 24.2 ± 1.8; Fig. 5*b*); again, this decrease was already significant at the first 3 months scoring interval ($P < 0.05$). Also FVC significantly decreased from 91.0 ± 1.9 to 58.0 ± 3.0, $P < 0.01$ (Fig. 5*d*).

Similar results were obtained for the MRC scale (140.7 ± 1.2 vs. 92.0 ± 5.3, $P < 0.01$), starting from the 6th month ($P < 0.05$) (Fig. 5*e*).

When we compared the groups at the end of the follow up, the mean decrement in the normalized Norris score was 46.1% in patients receiving riluzole only and 10.6% in those receiving lithium. Likewise, the decrease was more marked with respect to the baseline in the normalized ALSFRS-R in patients receiving riluzole only compared with lithium (39.8% vs. 14.3%). This was comparable for MRC, which decreased by 34.6% and 18.0%, in riluzole only- and lithium-treated patients, respectively.

In the Fig. 5*f* the FVC breakdown between lithium- and riluzole-treated patients is shown, and in Fig. 5*g* this is further detailed for the bulbar form of the disease.

Discussion

Our study indicates that lithium delays ALS progression in human patients. In fact, all subjects treated with lithium were alive at the end of the follow up (15 months), and their quality of life, as measured by SF-36, was not modified. By contrast, ≈30% of the patients receiving riluzole died during the study. The decreases we observed in the ALS-FRS-R and Norris scales were not statistically significant in the group treated with lithium. The delay in disease progression was also assessed more objectively by quantitative measurement of the muscle strength (by the MRC scale) and the preservation of the pulmonary function (by FVC). By contrast, the disease progressed markedly in the control group from the 3rd month of evaluation.

The analysis in the G93A mice showed that lithium delayed cell death within lamina IX and cranial MN while it increased the number of lamina VII Renshaw-like neurons above control values. In addition, lithium decreased reactive gliosis, rescued spinal cord mitochondria, and produced a marked regression of alpha-synuclein, ubiquitin, and SOD1 aggregates. This latter finding suggests that an increased removal of the mutated SOD1 may contribute to the improvement we observed in G93A mice. Thus, lithium affects multiple targets, all of which are likely to contribute to the improvement of ALS. Although not yet explored, numerous data associate autophagy with ALS. Apart from the autophagy impairment we found in the SOD1 model, another form of fALS, which is characterized by a mutation of dynein (38), likely depends on autophagy failure. In fact, now we know that dynein is critical for delivering the autophagosomes to lysosome to remove protein aggregates (22). In keeping with this observation, mutations in the dynein gene cause an autophagy impairment and reduce the clearance of aggregates (39). Another point mutation in the gene coding for dynactin, which participates in the dynamic of phagosomes, is responsible of fALS (40). Another form of fALS is caused by a mutation in the ALS 2 gene, i.e., the protein alsin (41), which is implicated in endosome trafficking. Interestingly, SOD1 is degraded by the autophagy pathway (42).

Thus, a convergence of different etiologies to produce an impairment of the endosomal–lysosomal autophagy pathway in producing MN disease is plausible. This pathway is strongly regulated by IP3 levels, which acts as an endogenous autophagy inhibitor, whereas lithium, by blocking IP3 activity, is a strong promoter of autophagy (18, 43), as confirmed in the present study at the level of the MN *in vivo*. Again, in primary MN cell cultures, we observed that lithium promoted autophagy at doses (1 mM) corresponding to those necessary to inhibit the IP3 turn-over (16, 17), whereas increasing the dose of lithium up to 2–3 mM (thus recruiting the inhibitory activity on GSK3 beta) produced a dramatic increase in cell adhesion. A defective endosomal–lysosomal autophagy pathway (due to either a primary defect in this pathway or dysfunctional mitochondria) could be the common denominator in various forms of ALS. Increasing autophagy to induce neuroprotection was recently fostered by Rubinsztein (44), who discussed the issue of the risk of decreasing mitochondria as a side-effect. In the present study, we demonstrate that lithium, although it increases autophagy, concomitantly produces a marked increase in the number of newly formed undamaged mitochondria. These effects, together with an increase in the number of neurons in lamina VII, may underlie the neuroprotective effects of lithium in the mouse model. A slight protective effect of lithium was recently described by Shin *et al.* in G93A mice (51). In this article, high doses of the compound were used, which may lead to additional effects (some of which may be detrimental for MN; see above). In fact, in their study, despite a delayed disease onset, the duration of disease was shortened by lithium administration.

At the same time, focusing only on autophagy may be misleading given the multiple targets we found in the present work. For instance, the suppression of glial cells activation we demonstrated in the spinal cord of lithium-treated G93A mice may be critical in view of the recent reports of the detrimental role of glia on MN survival (6–8). This point is addressed further in *Discussion* in *SI Text*, which also provides a multifaceted perspective on the potential mechanisms underlying the effects produced by lithium in ALS.

Materials and Methods

Genetic Background and Breeding Protocol of G93A Mice. All of the experiments were carried out in compliance with European Council Directive 86/609/EEC for the use and care of laboratory animals. B6SJL-TgN(SOD1-G93A)1Gur mice expressing the human G93A Cu/Zn superoxide dysmutase (SOD1) mutation were obtained from The Jackson Laboratory. For details, see *Methods* in *SI Text*.

Methods. ***Behavior.*** Behavioural observations were made by blind observers once a day for all animal groups ($n = 20$ per group). For details, see *Methods* in *SI Text*.

Tissue preparation staining procedures and histological analyses. See *Methods* in *SI Text*.

Electron microscopy. Mice ($n = 10$ from each group, WT, WT plus lithium, G93A, and G93A plus lithium) were perfused and spinal cords were maintained *in situ* immersed in fixative solution (2% paraformaldehyde/0.1% glutaraldehyde). For details, see *Methods* in *SI Text*.

Primary neuronal cultures, immunocytochemistry, cell labeling, and toxicity. Mixed spinal cord cultures were prepared from 13-day-old embryos of a control female mated with a G93A male as described in ref. 37. Three days after plating, AraC (10 μM) was added. For details, see *Methods* in *SI Text*.

SH-SY5Y cell lines and treatments. Human neuroblastoma SH-SY5Y cell line was obtained from the American Type Culture Collection (ATCC) and cultured under standard culture conditions. Cells were seeded and cultivated for 24 h before starting the treatments with 1 mM lithium carbonate (Sigma), 50 mM asparagine (Sigma), and 400 nM rapamycin. Treatments lasted 72 h. We changed the medium and reread the substances every 24 h. Detailed protocols are described in *Methods* in *SI Text*.

Statistical analysis. Data are given as mean ± SEM. Group mean values were compared by ANOVA, followed by post hoc testing.

Clinical Trial. ***Study design and patients.*** We conducted a 15-month parallel-group randomized study of adults with ALS, diagnosed according to the El Escorial revised diagnostic criteria (47), with a disease duration of <5 years.

The study protocol was approved by the Neuromed IRCCS Ethical Committee, and all subjects provided written informed consent. Initial statistical analysis determined that at least 40 subjects were needed to determine, with a 95% confidence interval, a survival increase >6 months.

The present study was performed on 44 patients (20 male and 24 female). No familial case was present. Eleven patients presented the bulbar form of the disease, and the remaining presented the classic onset. Sixteen patients (eight male and eight female, four of whom had the bulbar form) were randomly selected to receive riluzole (Rilutek 50 mg, 1 tablet × 2/day) plus lithium (Carbolithium; two daily 150-mg doses of lithium carbonate), and the remaining (12 male and 16 female, 7 of whom had the bulbar form) received riluzole only (48). In this way, we carefully matched lithium-treated and control patients for bulbar forms and FVC at the time of their inclusion in the study. In particular, the FVC values were 89 ± 10 and 91 ± 10 for lithium-treated and control patients, respectively. Again, the bulbar forms were distributed similarly between the groups (4/16 = 25%) in the treated group and (7/22 = 32%) for controls. One physician was not blind to group assignment; however, clinical evaluation, measurement of FVC, and data analysis were conducted by other physicians who were blind to group identities (single-blind study). In this way, the first physician was able to monitor lithium concentration and to adjust the daily dose from 300 mg up to 450 mg daily when lithium plasma levels were <0.4 mEq/liter. In fact, the daily dose was selected to reach a plasma range of 0.4–0.8 mEq/liter.

Compliance and adverse effects were monitored throughout the study period. Subjects were assessed six times (at baseline and every 3 months for 15 months). The primary endpoint of the present study was the survival rate. The secondary outcomes measured changes in global function, as scored by the ALSFRS-R (49), a widely used and extensively validated functional scale for ALS (normal score, 48); and by the Norris ALS scale. This disability score includes evaluation of the functioning of upper and lower limbs, also taking into

account bulbar function. This score uses 34 items rated with a value from 0 to 3, and the normal score is 100. Quality of life (SF-36) (50) was also evaluated. In parallel, we assessed the disease progression with more objective measures, such as quantitative segmental muscle strength (by the MRC scale) and the pulmonary function (FVC). The use of these combined approaches is very useful in small brief clinical trials (see *Discussion* in *SI Text* for a comparison of reliability between different scales).

Data analysis. The case analysis used all subjects who entered in the protocol study. Statistical analysis included a descriptive analysis of each group's data. Kolmogorov–Smirnov test of normality was nonsignificant for all variables. Measures were compared every 3 months with respect to the baseline condition, using an ANOVA for repeated measures. Comparisons between the two groups' mean scores were made by using the unpaired *t* test and, if necessary, ANOVA, with Bonferroni as post hoc test. Survival analysis was performed by the Kaplan–Meier curve. The null hypothesis was rejected when $P \leq 0.05$ for all tests. Statistical analyses were performed by using MedCalc software (version 9.3.6.0). See *Methods* in *SI Text* for the detailed methods of the basic study.

1. Bruijn LI, Miller TM, Cleveland DW (2004) *Annu Rev Neurosci* 27:723–749.
2. Rosen DR (1993) *Nature* 362:59–62.
3. Gurney ME, Pu H, Chiu AY, Dal Canto MC, Polchow CY, Alexander DD, Caliendo J, Hentati A, Kwon YW, Deng HX, *et al.* (1994) *Science* 264:1772–1775.
4. Wong PC, Pardo CA, Borchelt DR, Lee MK, Copeland NG, Jenkins NA, Sisodia SS, Cleveland DW, Price DL (1995) *Neuron* 14:1105–1116.
5. Clement AM, Nguyen MD, Roberts EA, Garcia ML, Boillée S, Rule M, McMahon AP, Doucette W, Siwek D, Ferrante RJ, *et al.* (2003) *Science* 302:113–117.
6. Ferri A, Nencini M, Casciati A, Cozzolino M, Angelini DF, Longone P, Spalloni A, Rotilio G, Carrì MT (2004) *FASEB J* 11:1261–1263.
7. Di Giorgio FP, Carrasco MA, Siao MC, Maniatis T, Eggan K (2007) *Nat Neurosci* 5:608–614.
8. Nagai M, Re DB, Nagata T, Chalazonitis A, Jessell TM, Wichterle H, Przedborski S (2007) *Nat Neurosci* 5:615–622.
9. Martin LJ, Liu Z, Chen K, Price AC, Pan Y, Swaby JA, Golden WC (2007) *J Comp Neurol* 500:20–46.
10. Morrison BM, Gordon JW, Ripps ME, Morrison JH (1996) *J Comp Neurol* 373:619–631.
11. Shefner JM, Logigian EL (1998) *Electromyogr Clin Neurophysiol* 38:505–510.
12. Chuang DM, Chen RW, Chalecka-Franaszek E, Ren M, Hashimoto R, Senatorov V, Kanai H, Hough C, Hiroi T, Leeds P (2002) *Bipolar Disord* 4:129–136.
13. Ryves JW, Dalton EC, Harwood AJ, Williams RS (2005) *Bipolar Disord* 7:260–265.
14. Cappuccio I, Calderone A, Busceti CL, Biagioni F, Pontarelli F, Bruno V, Storto M, Terstappen GT, Gaviraghi G, Fornai F, *et al.* (2005) *J Neurosci* 25:2647–2657.
15. Busceti CL, Biagioni F, Aronica E, Riozzi B, Storto M, Battaglia G, Giorgi FS, Gradini R, Fornai F, Caricasole A (2007) *Epilepsia* 48:694–705.
16. Berridge MJ, Irvine RF (1989) *Nature* 341:197–205.
17. Berridge MJ, Downes CP, Hanley MR (1989) *Cell* 59:411–419.
18. Sarkar S, Floto RA, Berger Z, Imarisio S, Cordenier A, Pasco M, Cook LJ, Rubinsztein DC (2005) *J Cell Biol* 170:1101–1111.
19. Hara T, Nakamura K, Matsui M, Yamamoto A, Nakahara Y, Suzuki-Migishima R, Yokoyama M, Mishima K, Saito I, Okano H, *et al.* (2006) *Nature* 441:885–889.
20. Komatsu M, Waguri S, Chiba T, Murata S, Iwata J, Tanida I, Ueno T, Koike M, Uchiyama Y, Kominami E, *et al.* (2006) *Nature* 441:880–884.
21. Cuervo AM, Stefanis L, Fredenburg R, Lansbury PT, Sulzer D (2004) *Science* 305:1292–1295.
22. Rubinsztein DC, Ravikumar B, Acevedo-Arozena A, Imarisio S, O'Kane CJ, Brown SD (2005) *Autophagy* 1:177–178.
23. Nimchinsky EA, Young WG, Yeung G, Shah RA, Gordon JW, Bloom FE, Morrison JH, Hof PR (2000) *J Comp Neurol* 416:112–125.
24. Haenggeli C, Kato AC (2002) *Neurosci Lett* 335:39–43.
25. Thomas RC, Wilson VJ (1965) *Nature* 206:211–213.
26. Kim JS, Chang MY, Yu IT, Kim JH, Lee SH, Lee YS, Son H (2004) *J Neurochem* 89:324–336.
27. Chi L, Ke Y, Luo C, Li B, Gozal D, Kalyanaraman B, Liu R (2006) *Stem Cells* 24:34–43.
28. Bruijn LI, Becher MW, Lee MK, Anderson KL, Jenkins NA, Copeland NG, Sisodia SS, Rothstein JD, Borchelt DR, Price DL, *et al.* (1997) *Neuron* 18:327–338.
29. Mezey E, Dehejia A, Harta G, Papp MI, Polymeropoulos MH, Brownstein MJ (1998) *Nat Med* 4:755–757.
30. Watanabe M, Dykes-Hoberg M, Culotta VC, Price DL, Wong PC, Rothstein JD (2001) *Neurobiol Dis* 8:933–941.
31. Struewing IT, Barnett CD, Tang T, Mao CD (2007) *FEBS J* 274:2749–2765.
32. Munafo DB, Colombo MI (2001) *J Cell Sci* 114:3619–3629.
33. Kabeya Y, Mizushima N, Ueno T, Yamamoto A, Kirisako T, Noda T, Kominami E, Ohsumi Y, Yoshimori T (2000) *EMBO J* 19:5720–5728.
34. Hoyvik H, Gordon PB, Berg TO, Stramhaug PE, Seglen PO (1991) *J Cell Biol* 113:1305–1312.
35. Nixon RA (2006) *Trends Neurosci* 29:528–535.
36. Seglen PO, Gordon PB (1982) *Proc Natl Acad Sci USA* 79:1889–1892.
37. Spalloni A, Albo F, Ferrari F, Mercuri N, Bernardi G, Zona C, Longone P (2004) *Neurobiol Dis* 15:340–350.
38. Hafezparast M, Klocke R, Ruhrberg C, Marquardt A, Ahmad-Annuar A, Bowen S, Lalli G, Witherden AS, Hummerich H, Nicholson S, *et al.* (2003) *Science* 300:808–812.
39. Ravikumar B, Acevedo-Arozena A, Imarisio S, Berger Z, Vacher C, O'Kane CJ, Brown SD, Rubinsztein DC (2005) *Nat Genet* 37:771–776.
40. La Monte BH, Wallace KE, Holloway BA, Shelly SS, Ascaño J, Tokito M, Van Winkle T, Howland DS, Holzbaur EL (2002) *Neuron* 34:715–727.
41. Yang Y, Hentati A, Deng HX, Dabbagh O, Sasaki T, Hirano M, Hung WY, Ouahchi K, Yan J, Azim AC, *et al.* (2001) *Nat Genet* 29:160–165.
42. Kabuta T, Suzuki Y, Wada K (2006) *J Biol Chem* 281:30524–30533.
43. Criollo A, Maiuri MC, Tasdemir E, Vitale I, Fiebig AA, Andrews D, Molgó J, Díaz J, Lavandero S, Harper F, *et al.* (2007) *Cell Death Differ* 14:1029–1039.
44. Rubinsztein DC (2006) *Nature* 443:780–786.
45. Paxinos G, Franklin KBJ (2004) The Mouse Brain in Stereotaxic Coordinates (Academic, San Diego).
46. Lin L, Georgievska B, Mattsson A, Isacson O (1999) *Proc Natl Acad Sci USA* 96:12108–12113.
47. Brooks BR, Miller RG, Swash M, Munsat TL, World Federation of Neurology Research Group on Motor Neuron Diseases (2000) *Amyotroph Lateral Scler Other Motor Neuron Disord* 1:293–299.
48. Miller RG, Mitchell JD, Lyon M, Moore DH (2007) *Cochrane Database Syst Rev* 24:1:1–25.
49. Cedarbaum JM, Stambler N, Malta E, Fuller C, Hilt D, Thurmond B, Nakanishi A (1999) *J Neurol Sci* 169:13–21.
50. Jenkinson C, Hobart J, Chandola T, Fitzpatrick R, Peto V, Swash ML (2002) *J Neurol* 249:178–183.
51. Shin J, Cho S, Lim H, Lee J, Lee Y, Noh J, Joo I, Kim K, Gwag B (2007) *Mol Pharmacol* 71:965–975.